Inorg. Chem. **2008**, *47*, 11108−11119

One-Dimensional Manganese Coordination Polymers Composed of Polynuclear Cluster Blocks and Polypyridyl Linkers: Structures and Properties

Svetlana G. Baca,*,† Iurii L. Malaestean,† Tony D. Keene,‡ Harry Adams,§ Michael D. Ward,§ Jürg Hauser,‡ Antonia Neels,|| and Silvio Decurtins*,‡

Institute of Chemistry, Academy of Sciences of Moldova, Academiei 3, MD-2028 Chisinau, R. Moldova, Department of Chemistry and Biochemistry, University of Bern, Freiestrasse 3, CH-3012 Bern, Switzerland, Department of Chemistry, University of Sheffield, Dainton Building, Sheffield, S7 3HF, U.K., and XRD Application Lab, CSEM Centre Suisse d'Electronique et de Microtechnique SA, Jaquet-Droz 1, Case Postale, CH-2002 Neuchâtel, Switzerland

Received July 28, 2008

The synthesis, crystal structures and magnetic properties of five new manganese compounds are reported. These include a linear trinuclear cluster $[Mn(II)_3(O_2CCHMe_2)_6(dpa)_2]\cdot 2MeCN$ (**1**) (dpa = 2,2′-dipyridylamine), a tetranuclear cluster $[Mn(II)_2Mn(III)_2O_2(O_2CCMe_3)_6(bpy)_2]$ (**3**) (bpy = 2,2′-bipyridine), and chain coordination polymers composed of cluster blocks such as Mn_3, Mn_3O, and Mn_4O_2 bridged by 2,2′-bipyrimidine (bpm) or hexamethylentetramine (hmta) ligands to give $([Mn(II)_3(O_2CCHMe_2)_6(bpm)]\cdot 2EtOH)_n$ (**2**), $[Mn(II)_2Mn(III)_2O_2(O_2CCHMe_2)_6(bpm)(EtOH)_4]_n$ (**4**), and $(([Mn(II)Mn(III)_2O(O_2CCHMe_2)_6(hmta)_2]\cdot EtOH)_n$ (**5**). The magnetic analysis of the compounds was achieved using a combination of vector coupling and full-matrix diagonalization methods. Susceptibility data for compound **1** was fitted using a vector coupling model to give $g = 2.02(1)$ and $2J/k_B = -5.38(2)$ K. To model the trimer chain, we used vector coupling for initial values of J_1 and then diagonalization techniques to estimate J_2 to give $g = 1.98(1)$, $2J_1/k_B = -3.3(1)$ K and $2J_2/k_B = -1.0(1)$ K by approximating the system to a dimer of trimers. The analysis of **3** was made difficult by the mixture of polymorphs and the difficulties of a three-*J* model, while for **4** an analysis was not possible because of the size of the computation and the relative magnitudes of the three couplings. Compound **5** was modeled using the same techniques as **2** to give $g = 1.99(1)$, $2J_1/k_B = +32.5(2)$ K, $2J_2/k_B = -16.8(1)$ K, and $2J_3/k_B = +0.4(1)$ K. The combination of techniques has worked well for compounds **2** and **5** and thus opens up a method of modeling complex chains.

Introduction

Coordination polymers are currently of great interest and represent an active area of coordination chemistry because of their special roles in fields such as ion exchange, gas storage, separation, sensor technology, magnets, optoelectronics, energy conversion and storage, and catalysis.[1] The most successful strategies for the design of coordination polymers are based on a building block approach. The assembly of one-, two-, or three-dimensional crystalline network structures can thus be achieved by choosing the desired combination of nodes and linkers.

Polynuclear metal carboxylate clusters are versatile frameworks for the generation of numerous molecular magnetic arrays. Moreover, some of them can behave as "single molecule magnets" (SMMs).[2,3] However, despite the characterization of many new polynuclear complexes, including those which behave as SMMs, little analogous work has been done to build coordination polymers having useful magnetic properties through the linking of individual metal clusters. Networks of metal clusters bridged by multifunctional ligands can result in more desirable magnetic properties than individual clusters in isolation.[1g] Christou et al. succeeded in the fabrication of the first one-dimensional (1D) chains

* To whom correspondence should be addressed. E-mail: sbaca_md@yahoo.com (S.G.B.), silvio.decurtins@iac.unibe.ch (S.D.).
† Academy of Sciences of Moldova.
‡ University of Bern.
§ University of Sheffield.
|| CSEM Centre Suisse d'Electronique et de Microtechnique SA.

10.1021/ic8014145 CCC: $40.75
Published on Web 10/29/2008

composed of mixed-valence trinuclear Mn_3O or nonanuclear Mn_9O_7 cluster blocks and 4,4′-bipyridine linkers.[4] Using Mn_6O_2 cluster building blocks, Yamashita et al. [5] have also synthesized a 1D chain assembly. A very interesting example in which three-dimensional Mn(II) complexes $[Mn_3(4\text{-aba})_6]_n$ (which individually exhibit both ferromagnetic and metamagnetic behavior) were linked by 4-aminobenzoic acid (4-Haba) has been reported by Hong et al.[6] A three-dimensional coordination polymer $[Mn_3(N_3)(nta)_4(H_2O)_2]_n$ [consisting of linear trinuclear Mn(II) subunits linked by nicotinate (nta)] which exhibits ferromagnetic intercluster couplings was reported by Chen et al.[7]

Despite the potential of this approach, the number of magnetic materials constructed in this way remains very small. Research in this field is motivated by the need for a better understanding of the fundamental principles that govern magnetic behavior, in particular when moving from isolated molecules to multidimensional solids. In this context, we have synthesized a new linear trinuclear Mn(II) complex $[Mn_3(O_2CCHMe_2)_6(dpa)_2]\cdot 2MeCN$ (**1**) (dpa = 2,2′-dipyridylamine) and a tetranuclear cluster $[Mn_4O_2(O_2CCMe_3)_6(bpy)_2]$ (**3**) (bpy = 2,2′-bipyridine) which have been linked into coordination networks using 2,2′-bipyrimidine (bpm) or hexamethylentetramine (hmta) as bridging ligands to generate $([Mn_3(O_2CCHMe_2)_6(bpm)]\cdot 2EtOH)_n$ (**2**), $[Mn_4O_2(O_2CCHMe_2)_6(bpm)(EtOH)_4]_n$ (**4**), and $(([Mn_3O(O_2CCHMe_2)_6(hmta)_2]\cdot EtOH)_n$ (**5**). In this paper we report their syntheses, structures, and magnetic properties.

Results and Discussion

Syntheses of Polynuclear Manganese Complexes. The discrete carboxylate clusters **1** and **3** were prepared by the reaction of manganese(II) isobutyrate or manganese(II) pivalate with appropriate N-containing ligands (Scheme 1). Complex $[Mn_3(O_2CCHMe_2)_6(dpa)_2]\cdot 2MeCN$ (**1**) consists of a homovalent Mn(II) trinuclear cluster with a linear core, containing two chelating 2,2′-dipyridylamine ligands, one on each terminal Mn(II) ion. Complex **3** is $[Mn_4O_2(O_2CCMe_3)_6(bpy)_2]$, a mixed-valent $Mn(II)_2Mn(III)_2$ tetranuclear cluster which contains a 2,2′-bipyridine chelating

Scheme 1

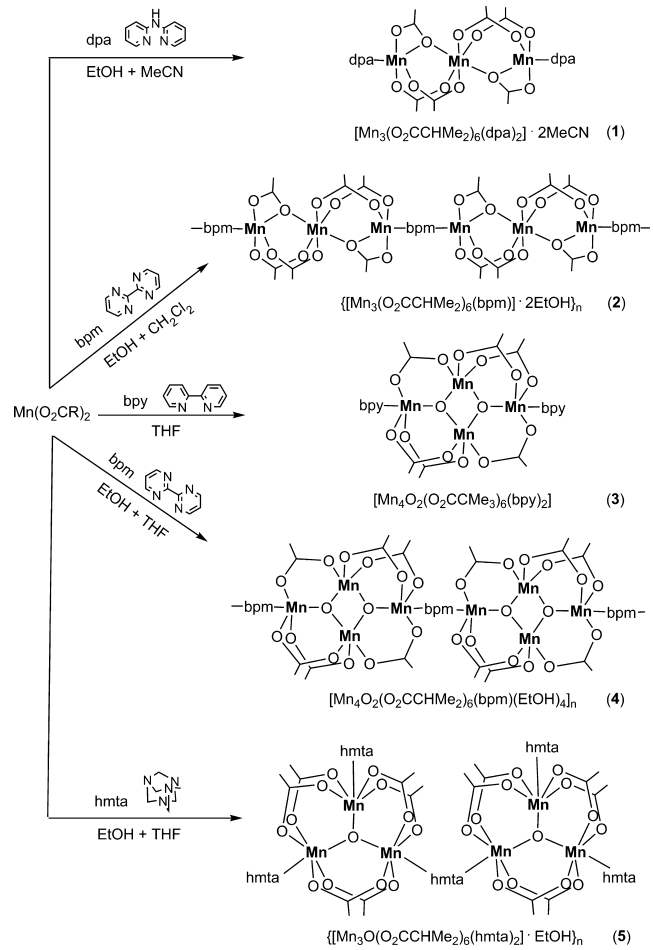

ligand on each of the Mn(II) centers. It is noteworthy that the use of simple Mn(II) salts in the reactions with polypyridyl ligands in alcohol solutions leads to a linear trinuclear core, as in **1**, which was prepared in MeCN/EtOH. This route was successfully explored resulting in the preparation of

(1) (a) Batten, S. R.; Robson, R. *Angew. Chem., Int. Ed.* **1998**, *37*, 1460. (b) Hagrman, P. J.; Hargman, D.; Zubieta, J. *Angew. Chem., Int. Ed.* **1999**, *38*, 2638. (c) Blake, A. J.; Champness, N. R.; Hubberstey, P.; Li, W.-S.; Withersby, M. A.; Schroder, M. *Coord. Chem. Rev.* **1999**, *183*, 117. (d) Robson, R. *J. Chem. Soc., Dalton Trans.* **2000**, 3735. (e) Eddaoudi, M.; Moler, D. B.; Li, H.; Chen, B.; Reineke, T. M.; O'Keeffe, M.; Yaghi, O. M. *Acc. Chem. Res.* **2001**, *34*, 319. (f) Moulton, B.; Zaworotko, M. J. *Chem. Rev.* **2001**, *101*, 1629. (g) Moulton, B.; Zaworotko, M. J. *Curr. Opin. Solid State Mater. Sci.* **2002**, *6*, 117. (h) Janiak, Ch. *J. Chem. Soc., Dalton Trans.* **2003**, 2781. (i) Yaghi, O. M.; O'Keeffe, M.; Ockwig, N. W.; Chae, H. K.; Eddaoudi, M.; Kim, J. *Nature* **2003**, *423*, 705. (j) Cheetham, A. K.; Rao, C. N. R.; Feller, R. K. *Chem. Commun.* **2006**, 4780. (k) Mueller, U.; Schubert, M.; Teich, F.; Puetter, H.; Schierle-Arndt, K.; Pastre, J. *J. Mater. Chem.* **2006**, *16*, 626. (l) Andruh, M. *Chem. Commun.* **2007**, 2565. (m) Wang, B.; Cote, A. P.; Furukawa, H.; O'Keeffe, M.; Yaghi, O. M. *Nature* **2008**, *453*, 207.

(2) SMM. (a) Lis, T. *Acta Crystallogr.* **1980**, *36*, 2042. (b) Sessoli, R.; Tsai, H.-L.; Schake, A. R.; Wang, S.; Vincent, J. B.; Folting, K.; Gatteschi, D.; Christou, G.; Hendrickson, D. N. *J. Am. Chem. Soc.* **1993**, *115*, 1804. (c) Sessoli, R.; Gatteschi, D.; Caneschi, A.; Novak, M. A. *Nature* **1993**, *365*, 141. (d) Aubin, S. M. J.; Wemple, M. W.; Adams, D. M.; Tsai, H.-L.; Christou, G.; Hendrickson, D. N. *J. Am. Chem. Soc.* **1996**, *118*, 7746.

(3) (a) Soler, M.; Rumberger, E.; Folting, K.; Hendrickson, D. N.; Christou, G. *Polyhedron* **2001**, *20*, 1365. (b) Price, D. J.; Batten, S. R.; Moubaraki, B.; Murray, K. S. *Chem. Commun.* **2002**, 762. (c) Brechin, E. K.; Boskovic, C.; Wernsdorfer, W.; Yoo, J.; Yamaguchi, A.; Sanado, E. C.; Concolino, T. R.; Rheingold, A. L.; Ishimoto, H.; Hendrickson, D. N.; Christou, G. C. *J. Am. Chem. Soc.* **2002**, *124*, 9710. (d) Soler, M.; Wernsdorfer, W.; Folting, K.; Pink, M.; Christou, G. *J. Am. Chem. Soc.* **2004**, *126*, 2156. (e) Murugesu, M.; Habrych, M.; Wernsdorfer, W.; Abboud, K. A.; Christou, G. *J. Am. Chem. Soc.* **2004**, *126*, 4766. (f) Tasiopoulos, A. J.; Vinslave, A.; Wernsdorfer, W.; Abboud, K. A.; Christou, G. *Angew. Chem., Int. Ed.* **2004**, *43*, 2117. (g) Sanudo, E. C.; Wernsdorfer, W.; Abboud, K. A.; Christou, G. *Inorg. Chem.* **2004**, *43*, 4137. (h) Murugesu, M.; Raftery, J.; Wernsdorfer, W.; Christou, G.; Brechin, E. K. *Inorg. Chem.* **2004**, *43*, 4203. (i) King, P.; Wernsdorfer, W.; Abboud, K. A.; Christou, G. *Inorg. Chem.* **2004**, *43*, 7315. (j) Tasiopoulos, A. J.; Wernsdorfer, W.; Abboud, K. A.; Christou, G. *Inorg. Chem.* **2005**, *44*, 6324. (k) King, P.; Wernsdorfer, W.; Abboud, K. A.; Christou, G. *Inorg. Chem.* **2005**, *44*, 8659. (l) Christou, G. *Polyhedron* **2005**, *24*, 2065. (m) Li, Y.; Wernsdorfer, W.; Clerac, R.; Hewitt, I. J.; Anson, C. E.; Powell, A. K. *Inorg. Chem.* **2006**, *45*, 2376. (n) Stamatatos, T. C.; Abboud, K. A.; Wernsdorfer, W.; Christou, G. *Angew. Chem., Int. Ed.* **2007**, *46*, 884. (o) Yang, C.-I.; Wernsdorfer, W.; Lee, G.-H.; Tsai, H.-L. *J. Am. Chem. Soc.* **2007**, *129*, 456. (p) Milios, C. J.; Inglis, R.; Bagai, R.; Wernsdorfer, W.; Collins, A.; Moggach, S.; Parsons, S.; Perlepes, S. P.; Christou, G.; Brechin, E. K. *Chem. Commun.* **2007**, 3476. (q) Bogani, L.; Wernsdorfer, W. *Nat. Mater.* **2008**, *7*, 179. (r) *Single-Molecule Magnets and Related Phenomena*; Winpenny, R., Ed.; Springer: Berlin/Heidelberg, 2006; Vol. *122*, p 262.

similar manganese(II) isobutyrates with 2,2′-bipyridine and 1,10′-phenanthroline (phen) ligands, [8] as well as linear trinuclear Mn(II) acetates.[9] In contrast, when THF was used as the solvent the tetranuclear heterovalent $Mn(II)_2Mn(III)_2$ complex **3** was formed. The addition of an ethanol solution of 2,2′-bipyrimidine (bpm) to manganese(II) isobutyrate in CH_2Cl_2 gives directly the chain coordination polymer $[Mn_3(O_2CCHMe_2)_6(bpm)]\cdot 2EtOH)_n$ (**2**), which consists of linear trinuclear cluster units ($Mn_3(O_2CCHMe_2)_6$) linked by bridging bpm ligands. In contrast, using THF as solvent afforded instead $[Mn_4O_2(O_2CCHMe_2)_6(bpm)(EtOH)_4]_n$ (**4**) in which tetranuclear mixed-valent $Mn(II)_2Mn(III)_2$ units are linked into a polymeric 1D chain by bridging bpm ligands. Finally, using hexamethylenetetramine as a bis-monodentate bridging ligand, a mixed-valent coordination polymer $([Mn_3O(O_2CCHMe_2)_6(hmta)_2]\cdot EtOH)_n$ (**5**) was prepared in which μ-oxo trinuclear carboxylate units are connected in a 1D chain.

The IR spectra of all complexes **1**−**5** have strong and broad bands in the 1615−1570 and 1423−1416 cm^{-1} regions, arising from the asymmetric and symmetric vibrations of the coordinated carboxylate groups of the pivalate or isobutyrate ligands.[10] The values of $\Delta = \nu_{as}(CO_2) - \nu_s(CO_2)$, being 147−199 cm^{-1}, fall in the range of reported values for bridging coordination of carboxylate groups.[10a] The ν(C=N) stretching vibrations for the N-containing ligands such as dpa,[11] bpy, [12] and bpm[13] in complexes **1**−**4** are also observed in this region (1651−1587 cm^{-1}), and these overlap with the asymmetric stretching band of the carboxylates. In the case of complex **5**, two well-separated strong and sharp bands at 1251 and 1231, 1025 and 996 cm^{-1} can be assigned as the C−N stretching modes of the coordinated hmta.[14] In all compounds multiple bands in the 2970−2870 cm^{-1} region, along with bands in the 1484−1459 and 1384−1361 cm^{-1} regions, are due to C−H vibrations of the methyl groups of carboxylic acids. The spectrum of **1** exhibits medium-intensity bands in the 3213−3044 cm^{-1} region corresponding to the N−H stretching vibrations of dpa ligands. Finally, the infrared spectra of **2**, **4**, and **5** all show a broadband in the 3435−3413 cm^{-1} region, which corresponds to ν(O−H) of the hydroxyl groups of ethanol molecules.

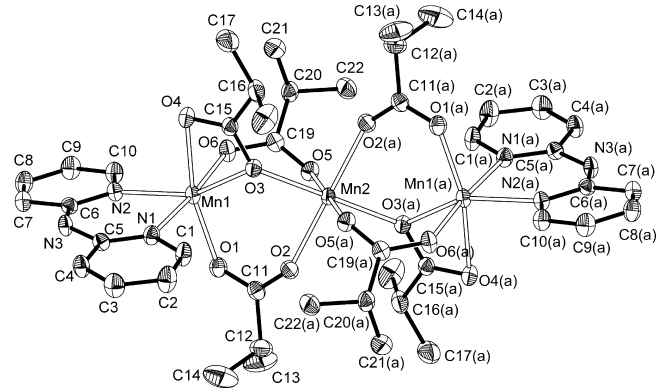

Figure 1. Asymmetric unit and selected symmetry equivalents of compound **1**. The letter "a" denotes the symmetry operation $-x + 2, -y, -z + 1$. Lattice solvent molecules and hydrogen atoms are omitted for clarity.

Description of Structures. $[Mn(II)_3(O_2CCHMe_2)_6(dpa)_2]\cdot 2MeCN$ (1). X-ray analysis revealed that complex **1** consists of a linear arrangement of three Mn(II) atoms bridged by six isobutyrate ligands, two terminal chelating dpa ligands, and two solvent MeCN molecules. The structure of **1** is displayed in Figure 1, and selected bond lengths and angles are listed in Table 1. Four isobutyrate ligands form bridges between the central and terminal Mn(II) atoms in the usual μ_2-1,3 coordination fashion. The other two isobutyrate ligands function as tridentate ligands in which one carboxylate oxygen atom O3 bridges two metal centers [Mn1 and Mn2], and the other oxygen atom O4 is coordinated only to Mn1, giving an overall μ_2-η^1:η^2 coordination mode. The Mn···Mn separation is 3.611(4) Å, a longer distance than that reported in analogous isobutyrate complexes with bpy [3.4894(3) Å] and phen [3.5312(3) Å] ligands.[8] For various acetate-bridged complexes with different terminal ligands the Mn···Mn distance can lie in the range of 3.370−3.716 Å;[9] in the benzoate-bridged complex the Mn···Mn separation is 3.588 Å.[15] Each Mn atom in **1** has a distorted octahedral geometry. The central Mn2 atom located on a crystallographic inversion center is coordinated by six oxygen carboxylate atoms from six different isobutyrate ligands with Mn−O lengths in the range 2.1554(14)−2.1881(16) Å. Two

(4) Eppley, H. J.; Vries, N.; Wang, S.; Aubin, S. M.; Tsai, H.-L.; Folting, K.; Hendrickson, D. N.; Christou, G. *Inorg. Chim. Acta* **1997**, *263*, 323.
(5) Nakata, K.; Miyasaka, H.; Sugimoto, K.; Ishii, T.; Sugiura, K.; Yamashita, M. *Chem. Lett.* **2002**, 658.
(6) Wang, R.; Gao, E.; Hong, M.; Gao, S.; Luo, J.; Lin, Z.; Han, L.; Cao, R. *Inorg. Chem.* **2003**, *42*, 5486.
(7) Chen, H.-J.; Mao, Z.-W.; Gao, S.; Chen, X.-M. *Chem. Commun.* **2001**, 2320.
(8) Baca, S. G.; Sevryugina, Yu.; Clerac, R.; Malaestean, Iu.; Gerbeleu, N.; Petrukhina, M. A. *Inorg. Chem. Commun.* **2005**, *8*, 474.
(9) Linear Mn_3 (a) Menage, S.; Vitols, S. E.; Bergerat, P.; Codjovi, E.; Kahn, O.; Girerd, J.-J.; Guillot, M.; Solans, X.; Calvet, T. *Inorg. Chem.* **1991**, *30*, 2666. (b) Rardin, R. L.; Poganiuch, P.; Bino, A.; Goldberg, D. P.; Tolman, W. B.; Liu, S.; Lippard, S. J. *J. Am. Chem. Soc.* **1992**, *114*, 5240. (c) Tsuneyoshi, K.; Kobayashi, H.; Miyamae, H. *Acta Crystallogr.* **1993**, *C49*, 233. (d) Tangoulis, V.; Malamatari, D. A.; Soulti, K.; Stergiou, V.; Raptopoulou, C. P.; Terzis, A.; Kabanos, T. A.; Kessissoglou, D. P. *Inorg. Chem.* **1996**, *35*, 4974. (e) Fernandez, G.; Corbella, M.; Mahia, J.; Maestro, M. A. *Eur. J. Inorg. Chem.* **2002**, 2502. (f) Asada, H.; Hayashi, K.; Negoro, S.; Fujiwara, M.; Matsushita, T. *Inorg. Chem. Commun.* **2003**, *6*, 193. (g) Li, Y.-G.; Lecren, L.; Wernsdorfer, W.; Clerac, R. *Inorg. Chem. Commun.* **2004**, *7*, 1281.
(10) (a) Deacon, G. B.; Philips, R. J. *Coord. Chem. Rev.* **1980**, *33*, 227. (b) Mehrotra, R. C.; Bohra, R. *Metal Carboxylates*; Academic Press: New York, 1983. (c) Nakamoto, K. *Infrared and Raman Spectra of Inorganic and Coordination Compounds*, Wiley, New York, 1986; p 236.
(11) Carballo, R.; Covelo, B.; Vazquez-Lopez, E. M.; Garcia-Martinez, E.; Castineiras, A.; Janiak, Ch. *Z. Anorg. Allg. Chem.* **2005**, *631*, 2006.
(12) (a) Thornton, D. A.; Watkins, G. M. *J. Coord. Chem.* **1992**, *25*, 299. (b) Czakis-Sulikowska, D.; Czylkowska, A. *J. Therm. Anal. Calorim.* **2005**, *82*, 69.
(13) (a) Julve, M.; Verdaguer, M.; De Munno, G.; Real, J. A.; Bruno, G. *Inorg. Chem.* **1993**, *32*, 795. (b) Andres, E.; De Munno, G.; Julve, M.; Real, J. A.; Lloret, F. *J. Chem. Soc., Dalton Trans.* **1993**, 2169. (c) Armentano, D.; De Munno, G.; Lloret, F.; Julve, M.; Curely, J.; Babb, A. M.; Lu, J. Y. *New J. Chem.* **2003**, *27*, 161. (d) Armentano, D.; De Munno, G.; Guerra, F.; Faus, J.; Lloret, F.; Julve, M. *Dalton Trans.* **2003**, 4626.
(14) Ahuja, I. S.; Singh, R.; Yadava, C. L. *Proc. Indian Acad. Sci. (Chem. Sci.)* **1983**, *92*, 59.
(15) Christou, G. *Acc. Chem. Res.* **1989**, *22*, 328.
(16) (a) Suezawa, H.; Yoshida, T.; Hirota, M.; Takahashi, H.; Umezawa, Y.; Honda, K.; Tsuboyama, S.; Nishio, M. *J. Chem. Soc., Perkin Trans.* **2001**, *2*, 2053. (b) Steiner, T. *Chem. Commun.* **1997**, 727. (c) Mascal, M. *Chem. Commun.* **1998**, 303.

Table 1. Selected Bond Distances (Å) and Angles (deg) in Complex **1**[a]

Mn1−O6	2.1207(18)	O3−Mn1−N1	91.33(7)
Mn1−O1	2.1557(18)	O6−Mn1−O4	86.64(7)
Mn1−N2	2.215(2)	O1−Mn1−O4	163.25(6)
Mn1−O3	2.2177(16)	N2−Mn1−O4	96.54(7)
Mn1−N1	2.256(2)	O3−Mn1−O4	56.95(6)
Mn1−O4	2.3764(18)	N1−Mn1−O4	89.01(7)
Mn2−O5	2.1554(16)	O5−Mn2−O5(a)	180.0
Mn2−O5(a)	2.1554(16)	O5−Mn2−O3(a)	92.34(6)
Mn2−O3(a)	2.1686(16)	O5(a)−Mn2−O3(a)	87.66(6)
Mn2−O3	2.1686(16)	O5−Mn2−O3	87.66(6)
Mn2−O2(a)	2.1881(16)	O5(a)−Mn2−O3	92.34(6)
Mn2−O2	2.1881(16)	O3(a)−Mn2−O3	180.00(6)
O6−Mn1−O1	95.06(7)	O5−Mn2−O2(a)	92.51(6)
O6−Mn1−N2	94.68(7)	O5(a)−Mn2−O2(a)	87.49(6)
O1−Mn1−N2	99.91(7)	O3(a)−Mn2−O2(a)	94.33(6)
O6−Mn1−O3	88.76(6)	O3−Mn2−O2(a)	85.67(6)
O1−Mn1−O3	106.37(6)	O5−Mn2−O2	87.49(6)
N2−Mn1−O3	153.09(7)	O5(a)−Mn2−O2	92.51(6)
O6−Mn1−N1	174.76(7)	O3(a)−Mn2−O2	85.67(6)
O1−Mn1−N1	89.94(7)	O3−Mn2−O2	94.33(6)
N2−Mn1−N1	82.90(7)	O2(a)−Mn2−O2	180.00(7)

[a] Symmetry transformations used to generate equivalent atoms: (a) $-x + 2, -y, -z + 1$.

(crystallographically equivalent) terminal manganese atoms [Mn1 and Mn1(a)] are in a distorted octahedral N_2O_4 environment, with four oxygen carboxylate atoms from three isobutyrate ligands [Mn−O distances range from 2.1207(18) to 2.3764(18) Å] and two nitrogen atoms of a chelating dpa molecule [Mn−N 2.215(2) and 2.256(2) Å]. The observed distortion from octahedral geometry at Mn1 and Mn1(a) is caused by the small bite angle of the chelating carboxylate group with O(3)−Mn(1)−O(4) of 56.95(6)°. Adjacent complex molecules are joined together through N−H···O hydrogen bonds [N···O distance, 2.989(3) Å] between the amine nitrogen atom N3 of the dpa ligand and the oxygen atom O1 [$x - 1/2, y, -z + 3/2$] of a carboxylate, resulting in a two-dimensional network (Figure 2). An additional long $\pi\cdots\pi$ interaction occurs between the aromatic ring C1C2C3C4C5N1 of the dpa ligand and the aromatic ring C6C7C8C9C10N2 of the adjacent complex (centroid−centroid distance is 4.063 Å, the interplanar angle is 23.16°, and the shortest distance between C5 and C10 [$x - 1/2, y, -z + 3/2$] is 3.5124(3) Å).

The solvent acetonitrile molecules fill the gaps between the layers of Mn(II) complexes (Supporting Information, Figure 1S) and are involved in weak hydrogen bonds. There are aliphatic−aromatic C−H···π interactions between the hydrogen [H23A] of the methyl group [C23] and an aromatic ring of dpa, with the shortest interatomic distance of C23−H23A···C10 [$1 - x, 1/2 + y, 3/2 - z$] = 2.791(2) Å (a typical aliphatic-aromatic interaction is in a range of 2.79−3.05 Å [16a]). Also there is a C−H···O contact of 2.340(5) Å involving a carboxylate group (C23−H23···O4 [$1 - x, 1/2 + y, 3/2 - z$] (typical C−H···O distances lie in the range 2.1−2.3 Å [16b]). There is a C−H···N contact of 2.655(3) Å with the N atom from the neighboring acetonitrile molecule, C23−H23B···N4 [$-1/2 + x, y, 3/2 - z$].[16c] Finally, N4 has weak contacts with H14C of the methyl group of the carboxylic acid [N4···H14C ($-1/2 + x, 1 + y, 3/2 - z$) = 2.703(7) Å] and with H3A of a dpa molecule [N4···H3A ($x, 1 + y, z$) = 2.735(1) Å].

$([Mn(II)_3(O_2CCHMe_2)_6(bpm)]\cdot 2EtOH)_n$ (2). A linear trinuclear Mn(II) aggregate bridged by six isobutyrate groups is the main structural unit in compound **2**; these trinuclear fragments are connected by bpm ligands into a 1D chain. The structure of complex **2** is displayed in Figure 3 and a packing diagram in Supporting Information, Figure 2S. Selected bond lengths and angles are listed in Table 2. Similar to compound **1**, the central atom Mn2 of each trinuclear unit is linked to the terminal manganese atoms Mn1 by three carboxylate groups in two different coordination modes: two of the isobutyrate groups in standard μ_2-bridging modes, and the third in a μ_2-η^1:η^2 coordination mode, forming a linear Mn1−Mn2−Mn1(a) sequence. In this trinuclear core the Mn···Mn separation of 3.743(5) Å is a longer than in **1**. The shortest interchain Mn···Mn distance is 7.0894(8) Å. The coordination polyhedron around each Mn atom is composed of the same donor atoms as in **1**. Mn2 is O_6-coordinated with Mn−O distances ranging from 2.164(2) to 2.222(2) Å; Mn1 adopts a highly distorted N_2O_4 octahedral geometry with Mn−O distances in the range 2.056(2)−2.289(2) Å, and two bpm nitrogen atoms [Mn1−N, 2.307(2) and 2.351(2) Å] complete the coordination sphere.

Solvent ethanol molecules are situated on either side of the plane of the bpm ligands (Supporting Information, Figure 3S) forming a short contact with the O4 atom of the isobutyrate ligand [C18−H18B···O4 ($1 + x, y, z$) = 2.812(4) Å] and an aliphatic−aromatic interaction between the hydrogen [H18C] of the methyl group [C18] and a bpm ring with the shortest interatomic distance of 2.296(6) Å [C18···C13 ($1 + x, y, z$) = 3.082(6) Å]. Atom O9 of the lattice solvent molecule is disordered which precludes any detailed discussion associated with its hydrogen bonding.

$[Mn(II)_2Mn(III)_2O_2(O_2CCMe_3)_6(bpy)_2]$ (3). X-ray single crystal structure determination reveals that complex **3** possesses planar Mn_4 units bridged by two μ_3-oxide atoms O1 and O1a. The structure of **3** is displayed in Figure 4 and a packing diagram in Supporting Information, Figure 4S. Selected bond distances and angles are in Table 3. Peripheral ligation is by six μ_2-O_2CCMe_3 and two terminal bpy groups. Each edge of the Mn_4 rhombus is bridged by either one or two μ_2-pivalate groups. Edges bridged by only one carboxylate group have a slightly longer Mn···Mn distance of 3.4756(7) Å than those bridged by two carboxylate groups [3.2808(7) Å]. The central Mn2···Mn2(a) separation is significantly shorter [2.7661(10) Å], consistent with the presence of two oxide bridges. The central μ_3-oxygen atoms are significantly displaced from the Mn_4 plane, by 0.601 Å. The $[Mn_4O_2]^{6+}$ core is mixed valence [$Mn(II)_2$, $Mn(III)_2$]. The two Mn(III) centers are assigned as the five-coordinate atoms Mn2 and Mn2(a) (atoms have a square-based pyra-

(17) Mn_4O_2 ($2Mn^{II}$, $2Mn^{III}$)(a) Vincent, J. B.; Christmas, C.; Chang, H.-R.; Li, Q.; Boyd, P. D. W.; Huffman, J. C.; Hendrickson, D. N.; Christou, G. *J. Am. Chem. Soc.* **1989**, *111*, 2086. (b) Kulawiec, R. J.; Crabtree, R. H.; Brudving, G. W.; Schulte, G. K. *Inorg. Chem.* **1988**, *27*, 1309. (c) Thorp, H. H.; Sarneski, J. E.; Kulawiec, R. J.; Bruving, G. W.; Crabtree, R. H.; Papaefthymiou, G. C. *Inorg. Chem.* **1991**, *30*, 1153.

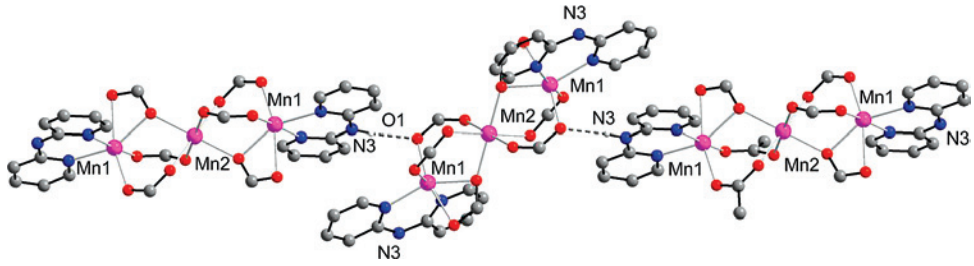

Figure 2. View of the hydrogen bonding in **1**. Hydrogen atoms are omitted for clarity [except N3−H3] and hydrogen bonds are indicated by dotted lines. Color code: Mn, pink; O, red; N, blue; C, gray.

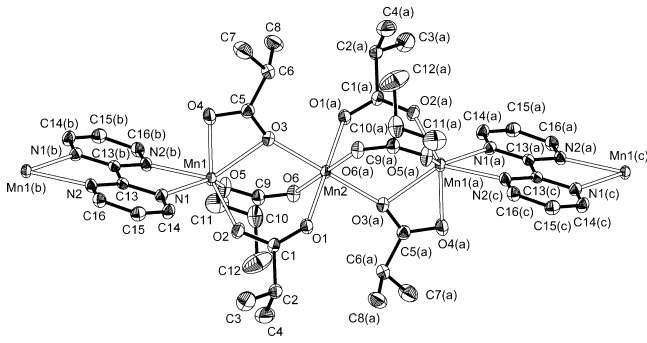

Figure 3. Asymmetric unit and selected symmetry equivalents of compound **2**. The letter "a" denotes the symmetry operation $-x, -y + 1, -z + 1$, the letter "b" $-x + 1, -y, -z + 1$, and the letter "c" $1 + x, -1 + y, z$. Lattice solvent molecules and hydrogen atoms are omitted for clarity.

Table 2. Selected Bond Distances (Å) and Angles (deg) in Complex **2**[a]

Mn1−O2	2.056(2)	O3−Mn1−N2(a)	131.60(8)
Mn1−O5	2.087(2)	O2−Mn1−N1	80.90(8)
Mn1−O4	2.238(2)	O5−Mn1−N1	141.38(8)
Mn1−O3	2.289(2)	O4−Mn1−N1	84.72(8)
Mn1−N2(a)	2.307(2)	O3−Mn1−N1	128.27(8)
Mn1−N1	2.351(2)	N2(a)−Mn1−N1	70.43(8)
Mn2−O6(a)	2.164(2)	O6(b)−Mn2−O6	180.00(12)
Mn2−O6	2.164(2)	O6(b)−Mn2−O1(b)	89.48(8)
Mn2−O1(b)	2.1650(19)	O6−Mn2−O1(b)	90.52(8)
Mn2−O1	2.1650(19)	O6(b)−Mn2−O1	90.52(8)
Mn2−O3	2.222(2)	O6−Mn2−O1	89.48(8)
Mn2−O3(b)	2.222(2)	O1(b)−Mn2−O1	180.0
O2−Mn1−O5	99.23(9)	O6(b)−Mn2−O3	92.13(8)
O2−Mn1−O4	126.64(10)	O6−Mn2−O3	87.87(8)
O5−Mn1−O4	122.32(10)	O1(b)−Mn2−O3	87.96(8)
O2−Mn1−O3	94.61(8)	O1−Mn2−O3	92.04(8)
O5−Mn1−O3	90.33(8)	O6(b)−Mn2−O3(b)	87.87(8)
O4−Mn1−O3	57.03(8)	O6−Mn2−O3(b)	92.13(8)
O2−Mn1−N2(a)	133.79(9)	O1(b)−Mn2−O3(b)	92.04(8)
O5−Mn1−N2(a)	83.21(8)	O1−Mn2−O3(b)	87.96(8)
O4−Mn1−N2(a)	86.70(9)	O3−Mn2−O3(b)	180.00(10)

[a] Symmetry transformations used to generate equivalent atoms: (a) $-x, -y + 1, -z + 1$ (b) $-x + 1, -y, -z + 1$.

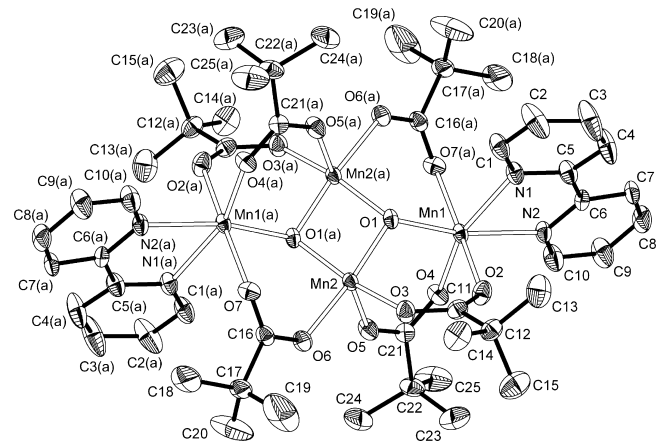

Figure 4. Asymmetric unit and selected symmetry equivalents of the tetranuclear cluster **3**. Hydrogen atoms are omitted for clarity. The letter "a" denotes the symmetry operation $-x + 1/2, -y + 1/2, -z + 2$.

Table 3. Selected Bond Distances (Å) and Angles (deg) in Complex **3**[a]

Mn1−O1	2.1017(19)	O4−Mn1−N2	87.16(8)
Mn1−O4	2.118(2)	O2−Mn1−N2	95.96(9)
Mn1−O2	2.169(2)	O7(a)−Mn1−N2	88.76(8)
Mn1−O7(a)	2.220(2)	O1−Mn1−N1	95.18(8)
Mn1−N2	2.268(2)	O4−Mn1−N1	158.70(8)
Mn1−N1	2.277(2)	O2−Mn1−N1	87.21(9)
Mn2−O1	1.8477(19)	O7(a)−Mn1−N1	88.67(9)
Mn2−O1(a)	1.856(2)	N2−Mn1−N1	71.70(9)
Mn2−O3	1.957(2)	O1−Mn2−O1(a)	83.34(9)
Mn2−O6	1.969(2)	O1−Mn2−O3	91.81(9)
Mn2−O5	2.095(2)	O1(a)−Mn2−O3	158.35(9)
Mn2−Mn2(a)	2.7666(9)	O1−Mn2−O6	168.71(9)
O1−Mn1−O4	106.04(8)	O1(a)−Mn2−O6	93.94(9)
O1−Mn1−O2	85.22(8)	O3−Mn2−O6	86.71(9)
O4−Mn1−O2	92.57(9)	O1−Mn2−O5	103.37(8)
O1−Mn1−O7(a)	88.83(8)	O1(a)−Mn2−O5	103.53(9)
O4−Mn1−O7(a)	93.57(8)	O3−Mn2−O5	98.12(9)
O2−Mn1−O7(a)	172.43(8)	O6−Mn2−O5	87.93(9)
O1−Mn1−N2	166.70(8)		

[a] Symmetry transformations used to generate equivalent atoms: (a) $-x + 1/2, -y + 1/2, -z + 2$.

midal geometry), while the two Mn(II) centers are assigned as the six-coordinate atoms Mn1 and Mn1(a) (atoms have a distorted octahedral geometry). Note also that the Mn−ligand distances are longer for the Mn(II) sites of the complex [Mn−O = 2.1017(19)−2.220(2); Mn−N = 2.268(2) and 2.277(2) Å] than those for Mn(III) sites [Mn−O = 1.8477(19)−2.095(2) Å] as expected for the lower oxidation state; and also confirmed by bond valence sum (BVS) calculations (Supporting Information, Table 1S). Complex **3** is an addition to the family of tetranuclear manganese complexes with mixed-valence $Mn(II)_2Mn(III)_2O_2$ cores: $[Mn_4O_2(O_2CMe)_6(bpy)_2]$ first was obtained by Vincent et al.,[17a] and $[Mn_4O_2(O_2CCPh_3)_6(Et_2O)_2]$ was prepared by Crabtree et al.[17b,c]

$[Mn(II)_2Mn(III)_2O_2(O_2CCHMe_2)_6(bpm)(EtOH)_4]_n$ (4). X-ray analysis shows that complex **4** possesses tetranuclear units $[Mn_4O_2(O_2CCHMe_2)_6(EtOH)_4]$ bridged by bpm ligands forming a linear chain coordination polymer. One such Mn_4 unit has 2-fold symmetry with two crystallographically unique Mn atoms, Mn1 and Mn2; the adjacent Mn_4 unit is crystallographically independent and has no internal symmetry, with four independent Mn atoms, Mn3−Mn6. Thus, there are 1.5 Mn_4 units in the asymmetric unit of the crystal (Figure 5, a full numbering scheme is shown in Supporting

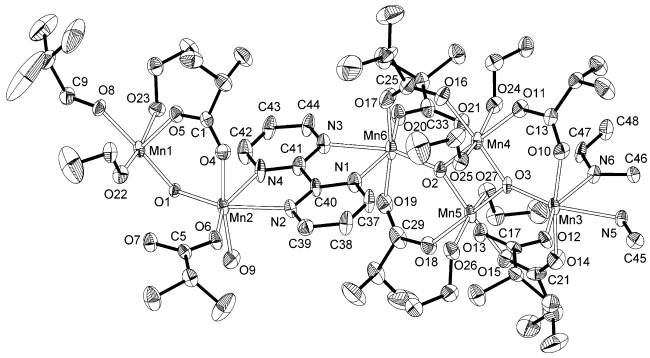

Figure 5. Asymmetric unit in compound **4.** Hydrogen atoms are omitted for clarity.

Information, Figure 5S). Selected bond distances and angles for cluster **4** are listed in Table 4, and a packing diagram for **4** is displayed in Supporting Information, Figure 6S. As in **3**, the structure of the Mn_4 core of complex **4** consists of four manganese atoms linked by two μ_3-oxo bridges lying on either side of the Mn_4 plane. The distance between the O1 atom and its symmetry-related O1(a) atom from the Mn1Mn2Mn1(a)Mn2(a) plane is equal to 0.217 Å, and atoms O2 and O3 are displaced from the Mn3Mn4Mn5Mn6 plane by 0.222 and 0.262 Å, respectively. However, in contrast to **3**, each edge of the Mn_4 rhombus in the core of **4** is bridged by only one isobutyrate. This is reflected in the Mn···Mn separations of 3.522(8)−3.550(7) Å, which are significantly longer than those observed when there are two bridging carboxylate groups [3.2808(7) Å in **3**]. The central Mn···Mn separations in each independent Mn_4 unit [Mn1···Mn1(a) and Mn4···Mn5] are 2.800(2) Å [2.7661(10) Å for **3**]. Each manganese atom is six coordinated and pseudo-octahedral. Mn1, Mn4, and Mn5 are O_6-coordinated by two μ-oxo atoms, two different isobutyrate ligands, and two ethanol ligands; the short Mn−O distances and irregular coordination geometries with one elongated axis (Table 4) are indicative of these ions being Mn(III) and displaying Jahn−Teller distortion, and as confirmed by bond-valence calculations (Supporting Information, Table 1S). The terminal manganese atoms of the Mn_4 units [Mn2, Mn3, and Mn6] have an N_2O_4 coordination environment arising from a chelating bpm ligand, three isobutyrate ligands (two bridging and one monodentate), and a μ_3-oxygen atom. On the basis of the longer Mn−O distances, Mn2, Mn3, and Mn6 can be assigned as Mn(II) centers. There are additional intrachain interactions between oxygen atoms O7, O13, and O21 of the isobutyrate groups and coordinated ethanol molecules (Figure 6). All hydrogen-bonding interactions are given in Supporting Information, Table 2S.

$([Mn(II)Mn(III)_2O(O_2CCHMe_2)_6(hmta)_2]\cdot EtOH)_n$ (5). X-ray analysis shows that complex **5** consists of μ-oxo trinuclear $[Mn_3O(O_2CCHMe_2)]$ clusters (Figure 7a) bridged by hexamethylentetramine units into a 1D chain polymer as shown in Figure 7b. Selected bond lengths and angles are listed in Table 5. In the μ-oxo trinuclear unit each Mn atom adopts a slightly distorted octahedral geometry and is coordinated by the central μ-oxygen atom, four oxygen atoms from bridging isobutyrate ligands, and a terminal hmta nitrogen atom. The central μ_3-oxygen atom is slightly displaced from the Mn_3 triangular plane [0.030(2) Å]. In the μ-oxo triangle the Mn1···Mn2 distance of 3.241(9) Å is

Table 4. Selected Bond Distances (Å) and Angles (deg) in Complex **4**[a]

Mn1−O1(a)	1.844(4)	O6−Mn2−N4	154.2(2)
Mn1O1	1.867(5)	O4−Mn2−N4	84.2(2)
Mn1−O5	1.982(5)	N2−Mn2−N4	69.8(2)
Mn1−O8	1.990(5)	O3−Mn3−O14	91.66(19)
Mn1−O22	2.268(5)	O3−Mn3−O12	121.59(18)
Mn1−O23	2.297(5)	O14−Mn3−O12	90.4(2)
Mn2−O1	2.067(5)	O3−Mn3−O10	92.66(19)
Mn2−O9	2.113(5)	O14−Mn3−O10	171.1(2)
Mn2−O6	2.122(5)	O12−Mn3−O10	94.0(2)
Mn2−O4	2.146(5)	O3−Mn3−N5	154.8(2)
Mn2−N2	2.348(6)	O14−Mn3−N5	85.8(2)
Mn2−N4	2.368(7)	O12−Mn3−N5	83.5(2)
Mn3−O3	2.073(4)	O10−Mn3−N5	86.97(19)
Mn3−O14	2.115(5)	O3−Mn3−N6	84.88(19)
Mn3−O12	2.134(5)	O14−Mn3−N6	90.3(2)
Mn3−O10	2.161(5)	O12−Mn3−N6	153.5(2)
Mn3−N5	2.350(6)	O10−Mn3−N6	82.3(2)
Mn3−N6	2.366(6)	N5−Mn3−N6	70.1(2)
Mn4−O3	1.841(5)	O3−Mn4−O2	82.0(2)
Mn4−O2	1.853(5)	O3−Mn4−O16	173.9(2)
Mn4−O16	1.978(5)	O2−Mn4−O16	97.2(2)
Mn4−O11	1.989(5)	O3−Mn4−O11	96.1(2)
Mn4−O25	2.269(5)	O2−Mn4−O11	172.7(2)
Mn4−O24	2.313(5)	O16−Mn4−O11	85.5(2)
Mn5−O2	1.852(5)	O3−Mn4−O25	92.0(2)
Mn5−O3	1.860(4)	O2−Mn4−O25	98.3(2)
Mn5−O15	1.975(5)	O16−Mn4−O25	82.1(2)
Mn5−O18	1.985(5)	O11−Mn4−O25	88.8(2)
Mn5−O27	2.261(5)	O3−Mn4−O24	98.7(2)
Mn5−O26	2.286(5)	O2−Mn4−O24	91.7(2)
Mn6−O2	2.070(5)	O16−Mn4−O24	87.4(2)
Mn6−O17	2.117(6)	O11−Mn4−O24	81.7(2)
Mn6−O20	2.131(6)	O25−Mn4−O24	166.36(19)
Mn6−O19	2.147(6)	O2−Mn5−O3	81.5(2)
Mn6−N3	2.342(6)	O2−Mn5−O15	175.6(2)
Mn6−N1	2.368(7)	O3−Mn5−O15	97.3(2)
O1(a)−Mn1−O1	82.1(2)	O2−Mn5−O18	96.7(2)
O1(a)−Mn1−O5	173.4(2)	O3−Mn5−O18	174.0(2)
O1−Mn1−O5	96.4(2)	O15−Mn5−O18	84.9(2)
O1(a)−Mn1−O8	97.3(2)	O2−Mn5−O27	92.0(2)
O1−Mn1−O8	174.8(2)	O3−Mn5−O27	98.24(19)
O5−Mn1−O8	84.8(2)	O15−Mn5−O27	83.9(2)
O1(a)−Mn1−O22	98.08(19)	O18−Mn5−O27	87.5(2)
O1−Mn1−O22	91.5(2)	O2−Mn5−O26	98.1(2)
O5−Mn1−O22	88.36(19)	O3−Mn5−O26	93.1(2)
O8−Mn1−O22	83.5(2)	O15−Mn5−O26	86.2(2)
O1(a)−Mn1−O23	91.73(19)	O18−Mn5−O26	81.5(2)
O1−Mn1−O23	98.98(19)	O27−Mn5−O26	165.8(2)
O5−Mn1−O23	82.16(19)	O2−Mn6−O17	91.5(2)
O8−Mn1−O23	86.2(2)	O2−Mn6−O20	119.8(2)
O22−Mn1−O23	166.56(18)	O17−Mn6−O20	92.0(2)
O1−Mn2−O9	92.46(19)	O2−Mn6−O19	93.0(2)
O1−Mn2−O6	120.52(18)	O17−Mn6−O19	170.0(2)
O9−Mn2−O6	90.1(2)	O20−Mn6−O19	93.5(2)
O1−Mn2−O4	92.87(19)	O2−Mn6−N3	154.8(2)
O9−Mn2−O4	172.2(2)	O17−Mn6−N3	89.4(2)
O6−Mn2−O4	92.1(2)	O20−Mn6−N3	85.3(2)
O1−Mn2−N2	155.0(2)	O19−Mn6−N3	82.8(2)
O9−Mn2−N2	88.1(2)	O2−Mn6−N1	85.1(2)
O6−Mn2−N2	84.5(2)	O17−Mn6−N1	87.1(2)
O4−Mn2−N2	84.7(2)	O20−Mn6−N1	155.1(2)
O1−Mn2−N4	85.2(2)	O19−Mn6−N1	84.3(2)
O9−Mn2−N4	90.6(2)	N3−Mn6−N1	69.8(2)
Mn1(a)−O1−Mn1	97.9(2)	Mn4−O2−Mn6	128.7(3)
Mn1(a)−O1−Mn2	129.3(2)	Mn4−O3−Mn5	98.3(2)
Mn1−O1−Mn2	128.8(2)	Mn4−O3−Mn3	128.2(2)
Mn5−O2−Mn4	98.2(2)	Mn5−O3−Mn3	128.1(2)
Mn5−O2−Mn6	128.6(2)		

[a] Symmetry transformations used to generate equivalent atoms: (a) $-x$, $-y+1$, $-z+2$.

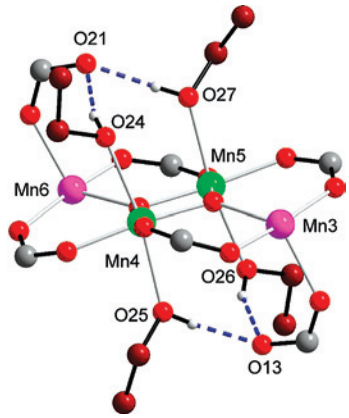

Figure 6. Fragment of the crystal structure of complex **4** showing hydrogen bonding interactions. $(Me)_2CH$ groups of isobutyric ligands and non hydrogen-bonding hydrogen atoms are omitted for clarity. Hydrogen bonds are indicated by dashed lines, while carbon atoms belonging to ethanol molecules are colored brown to aid differentiation from the acid groups. Color code: Mn(II), pink; Mn(III), green; O, red; N, blue; C, gray.

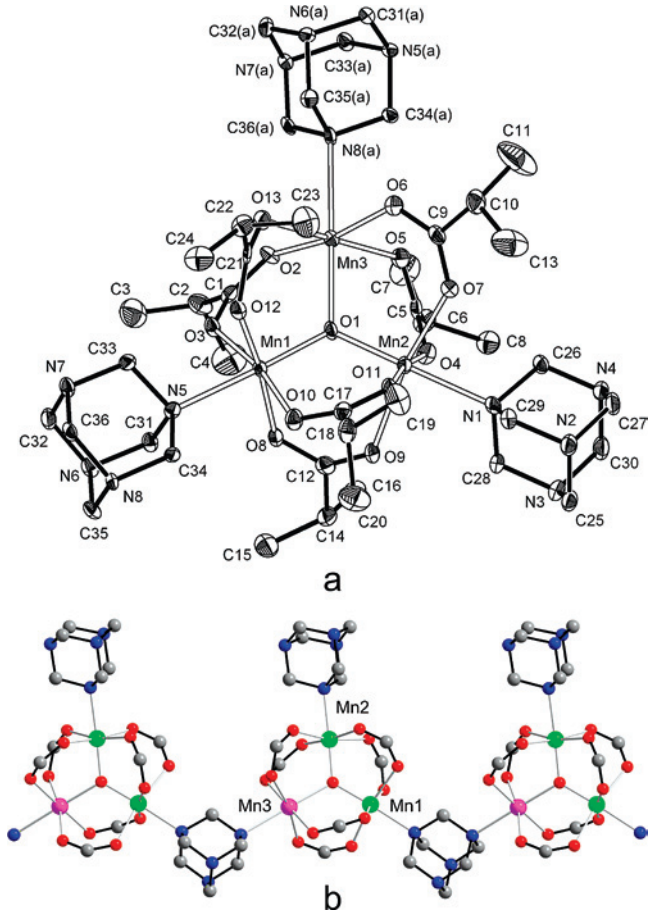

Figure 7. (a) Asymmetric unit and selected symmetry equivalents of compound **5**. The letter "a" denotes the symmetry operation $x + 1/2, -y + 1/2, z + 1/2$. Lattice solvent molecules and hydrogen atoms are omitted for clarity. (b) View of the chain in **5**. Lattice solvent molecules, hydrogen atoms, and the Me_2CH-groups of isobutyric acids are omitted for clarity. Color code: Mn(II), pink; Mn(III), green; O, red; N, blue; C, gray.

slightly shorter than the Mn1···Mn3 [3.432(9) Å] and Mn2···Mn3 [3.367(8) Å] distances. One hmta unit associated with each Mn_3 fragment is bridging and propagates the polymeric structure, which links Mn1 and Mn3 atoms—the second hmta ligand [coordinated to Mn2 atom] is terminal, as shown in Figure 7b.

Table 5. Selected Bond Distances (Å) and Angles (deg) in Complex **5**[a]

Mn1−O1	1.828(3)	O10−Mn1−N5	87.90(11)
Mn1−O8	1.980(3)	O1−Mn2−O11	94.28(12)
Mn1−O12	1.988(3)	O1−Mn2−O4	92.67(12)
Mn1−O3	2.144(3)	O11−Mn2−O4	171.35(12)
Mn1−O10	2.175(3)	O1−Mn2−O7	97.79(11)
Mn1−N5	2.196(3)	O11−Mn2−O7	85.38(12)
Mn2−O1	1.838(2)	O4−Mn2−O7	98.79(12)
Mn2−O11	1.957(3)	O1−Mn2−N1	177.44(13)
Mn2−O4	1.962(3)	O11−Mn2−N1	88.28(12)
Mn2−O7	2.150(3)	O4−Mn2−N1	84.77(12)
Mn2−N1	2.180(3)	O7−Mn2−N1	82.53(12)
Mn2−O9	2.181(3)	O1−Mn2−O9	92.48(11)
Mn3−O1	2.133(3)	O11−Mn2−O9	89.02(12)
Mn3−O6	2.142(3)	O4−Mn2−O9	85.53(12)
Mn3−O2	2.144(3)	O7−Mn2−O9	168.63(10)
Mn3−O5	2.157(3)	N1−Mn2−O9	87.43(12)
Mn3−O13	2.167(3)	O1−Mn3−O6	98.41(10)
Mn3−N8(a)	2.387(3)	O1−Mn3−O2	92.39(10)
O1−Mn1−O8	95.57(12)	O6−Mn3−O2	169.13(11)
O1−Mn1−O12	91.86(12)	O1−Mn3−O5	89.81(11)
O8−Mn1−O12	170.32(12)	O6−Mn3−O5	92.42(11)
O1−Mn1−O3	95.59(11)	O2−Mn3−O5	86.30(11)
O8−Mn1−O3	88.05(11)	O1−Mn3−O13	89.65(10)
O12−Mn1−O3	97.40(11)	O6−Mn3−O13	87.18(11)
O1−Mn1−O10	94.22(11)	O2−Mn3−O13	94.20(11)
O8−Mn1−O10	90.31(11)	O5−Mn3−O13	179.27(11)
O12−Mn1−O10	82.96(11)	O1−Mn3−N8(a)	178.87(11)
O3−Mn1−O10	170.16(11)	O6−Mn3−N8(a)	82.66(11)
O1−Mn1−N5	177.28(12)	O2−Mn3−N8(a)	86.55(11)
O8−Mn1−N5	86.10(12)	O5−Mn3−N8(a)	90.51(11)
O12−Mn1−N5	86.71(12)	O13−Mn3−N8(a)	90.04(11)
O3−Mn1−N5	82.31(11)		

[a] Symmetry transformations used to generate equivalent atoms: (a) $x + 1/2, -y + 1/2, z + 1/2$.

On the basis of the neutral charge of the $[Mn_3O(O_2CCMe_3)_6(hmta)_3]$ cluster, the Mn oxidation states in this complex must be $[Mn^{II}Mn^{III}_2O]^{6+}$. As expected for its lower oxidation state, the position of the Mn(II) atom can be assigned on the basis of its longer Mn−N and Mn−O bond distances compared with the Mn(III) atoms (Table 5) and as determined by bond-valence calculations (Supporting Information, Table 1S). From these data Mn3 is readily assigned as the Mn(II) center, whereas Mn1 and Mn2 are the Mn(III) centers.

Note that the nitrogen atom N7 of a bridging hmta ligand forms a hydrogen bond with an ethanol molecule of 2.873(5) Å [O14−H14A···N7 $(x + 1/2, -y + 1/2, z + 1/2)$] (Supporting Information, Figure 7S).

Magnetic Properties. The magnetic susceptibility plot of **1** (Figure 8) shows an increasing susceptibility with decreasing temperature, reaching a value of 2.49 $cm^3\ mol^{-1}$ at 1.86 K. The inverse susceptibility curve shows non-linear behavior across the temperature range, so a Curie−Weiss fit was not attempted. The $\chi T(T)$ plot (Figure 8) shows a decreasing value of χT with decreasing temperature, with a value of 13.075 $cm^3\ K\ mol^{-1}$ at 300 K (slightly lower than the spin-only value of 13.125 $cm^3\ K\ mol^{-1}$ for three Mn(II) with $g = 2.00$) and 4.60 $cm^3\ K\ mol^{-1}$ at 4.5 K. Below 4.5 K, a small upward curving feature appears.

This linear trimer system (Figure 9) can be modeled using the Hamiltonian in eq 1 and, using Kambe vector coupling, it is possible to derive an expression for fitting the susceptibility and χT data (couplings between terminal Mn atoms are discounted):

$$H = -2J(\boldsymbol{S}_A \cdot \boldsymbol{S}_B + \boldsymbol{S}_B \cdot \boldsymbol{S}_C) \quad (1)$$

The energy levels for this system[9a] are then inserted into the van Vleck equation (eq 2).

$$\chi = \frac{Ng^2\mu_B^2}{3k_BT} \cdot \frac{\sum S_T(S_T+1)(2S_T+1)\exp(-E/k_BT)}{\sum (2S_T+1)\exp(-E/k_BT)} \quad (2)$$

The resulting equation can then be used to simulate the behavior of **1**. Fitting this model to the χT data between 300−4.5 K gave $g = 2.02(1)$ and $2J/k_B = -5.38(2)$ K. In a linear $S = {}^5/_2$ trimer, an antiferromagnetic interaction leads to a ground state of $S_T = {}^5/_2$, and the value of χT at 4.5 K is consistent with this (4.60 cm^3 K mol^{-1} compared with the predicted value of 4.66 $cm^3 \cdot K \cdot mol^{-1}$ for $g = 2.02(1)$).

It is possible to model the magnetization of this system using eq 3[18,19]

$$M(T,B) = N\mu_B g \frac{\sum_{S\alpha} S\, B_S(gSx)\sinh[g(S+{}^1/_2)x]\exp[-E_{S\alpha}/(k_BT)]}{\sum_{S\alpha}\sinh[g(S+{}^1/_2)x]\exp[-E_{S\alpha}/(k_BT)]} \quad (3)$$

where B_S is the Brillouin function, $x = \mu_B B/(k_BT)$, and $E_{S\alpha}$ denotes the zero-field energy levels.

The χT model was more sensitive to changes in g- and J-values, so the values obtained from that fitting were used to model the magnetization. The calculated magnetization (Supporting Information, Figure 8S) shows good agreement with the data, and the difference between the curves is within experimental error. The field range covered in the measurement shows the alignment of the ground-state $S_T = {}^5/_2$ spins with the field.

The magnetic susceptibility plot of **2** (Figure 10) shows an increasing susceptibility on cooling with a maximum occurring at 6.0 K with a value of 0.40 cm^3 mol^{-1}. The inverse susceptibility plot is non-linear throughout the temperature range, so a Curie−Weiss fit was not attempted. The $\chi T(T)$ plot (Figure 10) shows a decreasing value on cooling with a value of 12.363 cm^3 K mol^{-1} at 300 K (slightly lower than the spin-only value of 13.125 cm^3 K mol^{-1} for three Mn(II) with $g = 2.00$), and falling well below the value expected for $S_T = {}^5/_2$ non-interacting trimers in the ground state at low temperature.

Considering the maximum in χ and the decreasing value of χT through the temperature range, it can be seen that the predominant interactions in **2** are antiferromagnetic. To the best of our knowledge, the chain structure of linear Mn_3 clusters linked by the bipyrimidine bridges in **2** has not been described elsewhere, and no model to describe the susceptibility of the system could be found. An attempt to model the low temperature data with the Fisher classical chain equation for an $S = {}^5/_2$ Heisenberg chain gave a poor fit and unreasonable g- and J-values. The main two reasons behind this are that it is unlikely that all the trimeric units are in the $S_T = {}^5/_2$ ground state over a wide enough temperature range in which to use the model, and also that for this approximation to work, the inter- and intracluster couplings would have to be quite similar. Next an attempt to model the magnetic susceptibility data using the linear $S = {}^5/_2$ trimer with a Mean Field Theory (MFT) correction was made, but this too resulted in a poor fit and unreasonable values. This was not surprising as MFT methods do not work well in general for 1D materials.

Another option was to make an approximation using a system of two linear clusters joined in a ring (Figure 9) and to calculate its properties using exact numerical diagonalization techniques. Limits in computing power meant that

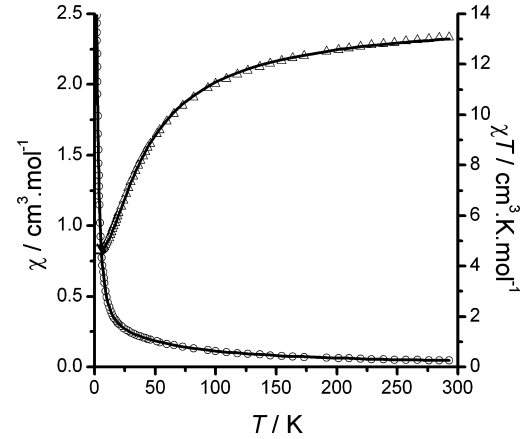

Figure 8. Plot of $\chi(T)$ (circles) for **1** with fit to trimer model and $\chi T(T)$ (triangles) with fit where $g = 2.02(1)$ and $2J/k_B = -5.38(2)$ K.

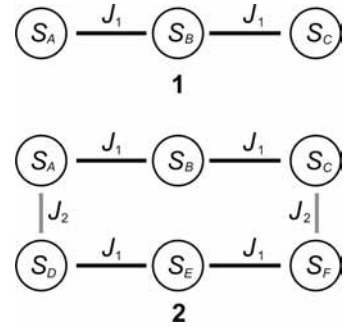

Figure 9. Coupling diagrams for **1** and **2**.

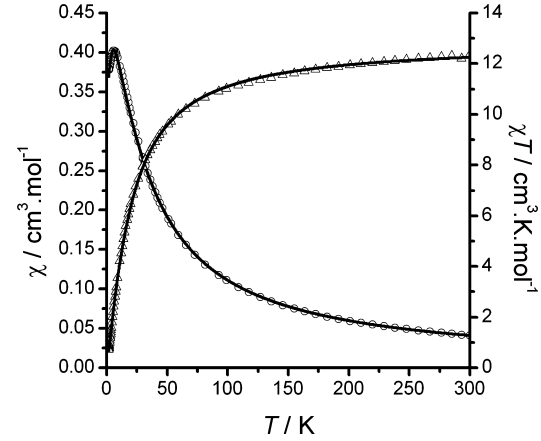

Figure 10. Plot of $\chi(T)$ (circles) for **2** with fit to trimer model and $\chi T(T)$ (triangles) with fit where $g = 1.98(1)$ and $2J_1/k_B = -3.3(1)$ K and $2J_2/k_B = -1.0(1)$ K.

(18) Waldmann, O. *Phys. Rev. B.* **2000**, *61*, 6138.
(19) Waldmann, O.; Güdel, T. L.; Kelly, T. L.; Thompson, L. K. *Inorg. Chem.* **2006**, *45*, 3295.

Table 6. Comparison of the Mn···Mn Distances (Å) and Magnetic Interaction ($2J$)[a]

complex	d Mn···Mn/Å	$2J/k_B$/K	reference
1	3.611(1)	−5.34(3)	this work
2	3.7449(1)	−3.39(1)	this work
$[Mn_3(4\text{-aba})_6]_n$	3.425	−6.48	6
$[Mn_3(O_2CHMe_2)_6(phen)_2]$	3.5312	−4.62	8
$[Mn_3(O_2CHMe_2)_6(bpy)_2]$	3.4894	−5.34	8
$[Mn_3(O_2CMe)_6(bpy)_2]$	3.614	−6.34	9a
$[Mn_3(O_2CMe)_6(pybim)_2]$	3.558	−5.5	9d
$[Mn_3(O_2CH_2Cl)_6(bpy)_2]$	3.624	−5.50	9e

[a] pybim - 2-2-pyridyl(benzimidazole); 4-aba - 4-aminobenzoic acid.

only two clusters could be used in the calculations as the Hilbert space for three clusters exceeds 10.1 million, so this model will be only approximate. The Hamiltonian for this system is described in eq 4

$$H = -2J_1(S_A \cdot S_B + S_B \cdot S_C + S_D \cdot S_E + S_E \cdot S_F) - 2J_2(S_A \cdot S_D + S_C \cdot S_F) \quad (4)$$

The refinement of the g, J_1, and J_2 values was carried out by visually inspecting the fit against the $\chi(T)$ and $\chi T(T)$ data and varying the parameters accordingly. Initial parameters were obtained from fitting the $\chi(T)$ data above 50 K with the linear trimer equation to give $g = 1.99$ and $2J_1/k_B = -3.75$ K. The best fit was obtained with $g = 1.98(1)$, $2J_1/k_B = -3.3(1)$ K and $2J_2/k_B = -1.0(1)$ K (Figure 10). Despite the approximate nature of this model, the data is modeled remarkably well to low temperature and only deviates significantly from the data at ~2 K. Using the values obtained from the fit, the magnetization curve (Supporting Information, Figure 9S) could be calculated using eq 3, which gives a good fit below 1.75 T but slightly overestimates the data above this.

The difference in intracluster coupling between **1** and **2** is likely due to the increased Mn−Mn and Mn−O−Mn distances (Table 6) as superexchange mechanisms are very sensitive to the distance between spin carriers through the coupling pathways and the Mn−O−Mn pathway is likely to give a stronger interaction than through the carboxylate bridges. The intracluster coupling constants are similar to previously reported compounds with the same trimer structure,[8,9a] and the intercluster coupling in **2** is also within the range found for Mn−bpym−Mn bridges.[20]

The magnetic susceptibility of **3** shows an increasing value on cooling, reaching 2.35 $cm^3\ mol^{-1}$ at 1.86 K (Figure 11). The inverse susceptibility plot shows non-linear behavior over the whole temperature range, so a Curie−Weiss fit was not attempted. The $\chi T(T)$ plot (Figure 11) shows a decreasing product on cooling with a value at 300 K of 8.49 $cm^3\ K\ mol^{-1}$. This is substantially below the value expected for an uncoupled $Mn(II)_2Mn(III)_2$ system ($\chi T = 14.75$ for $g = 2$).

Inspection of the structure reveals that the Mn(III) orbital bonding to the bridging oxygen atoms is the non-magnetic $d_{x^2-y^2}$ orbital so there will be no overlap of magnetic orbitals between the Mn(III) pair or from the Mn(III) to the Mn(II) atoms through this bridge. However, the bridging carboxylate

(20) Thétiot, F.; Triki, S.; Sala-Pala, J.; Golhen, S. *Inorg. Chim. Acta* **2005**, *358*, 3277, and the references therein.

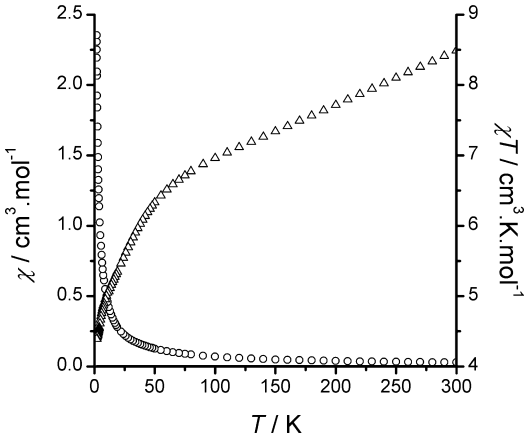

Figure 11. Plot of $\chi(T)$ (circles) and $\chi T(T)$ (triangles) for **3**.

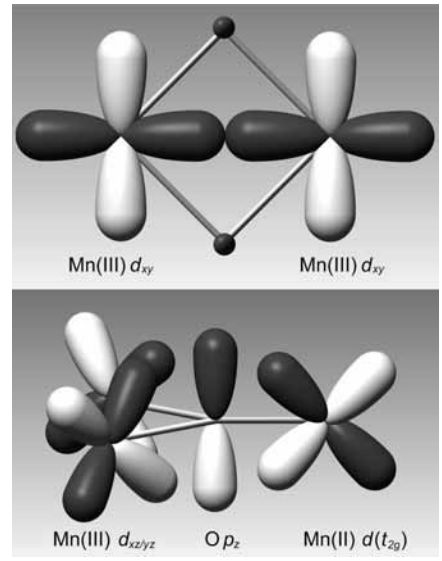

Figure 12. Representation of the magnetic orbital overlaps resulting in superexchange in **3** and **4**: (a) direct overlap of the Mn(III) d_{xy} orbitals and (b) overlap of the Mn(III) $d_{xz/yz}$, O p_z orbitals, and an orbital of the Mn(II) t_{2g} set.

connects the magnetic d_{z^2} of the Mn(III) atom to an orbital from the e_g set on the Mn(II) atom, thus presenting a superexchange pathway. Given the short Mn(III)−Mn(III) distance [2.767(3) Å] there should be some direct overlap of the d_{xy} orbitals (Figure 12a) and therefore a direct exchange interaction. In addition, the d_{xz} and d_{yz} orbitals can interact with the oxygen p_z orbital to produce a π-overlap and thus a superexchange pathway which also interacts with a magnetic orbital of the t_{2g} set on the Mn(II) atoms (Figure 12b). This combination of magnetic orbital overlaps produces a system where the Mn(III)−Mn(II) interactions are not equal (Figure 13)

$$H = -2J_1(S_A \cdot S_B) - 2J_2(S_A \cdot S_C + S_B \cdot S_D) - 2J_3(S_A \cdot S_D + S_B \cdot S_C) \quad (5)$$

This particular system cannot be modeled using Kambe vector coupling as there is no combination of spin pairs that allows the total spin of the system to be described. The low value of χT at 300 K and the initial slope in the $\chi T(T)$ data also imply that J_1 is considerably larger than the other

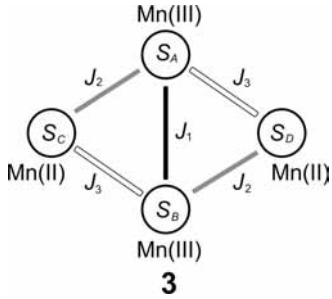

3

Figure 13. Coupling diagram for **3**. For compound **4**, $J_2 = J_3$.

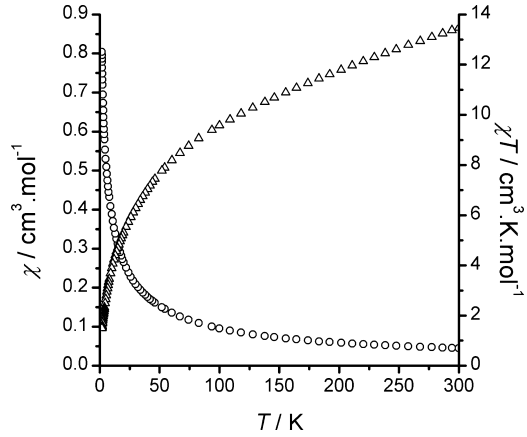

Figure 14. Plot of $\chi(T)$ (circles) and $\chi T(T)$ (triangles) for **4**.

couplings, which only appear to affect the plot below ~100 K.

Comparison of **3** with the system reported by Christou et al.[17a] shows that the couplings in the system are likely to be of a similar magnitude. Christou's data was modeled with a Hamiltonian that takes J_2 and J_3 to be equal and as such is not appropriate for this system, as can be seen from the low magnetic moment at 300 K and the very low g-value of 1.7 averaged over all four Mn atoms. Given that Mn(II) g-values deviate only fractionally from 2.00, this implies that the g-value of the Mn(III) atoms must be 1.4, which underlines the need to use the Hamiltonian in eq 5.

Taking these considerations into account, it is not easily possible to obtain coupling constants or g-values for this system and comparison to other systems would be not be appropriate as the couplings present are highly sensitive to changes in the M−O−M angle. Additionally, as **3** is a mixture of polymorphs, any small structural differences between them would affect the susceptibility curve which would be impossible to reproduce without knowing the exact ratio of the polymorphs.

The magnetization curve for **3** appears to show the curve tending to a value of 7 μ_B; however, it is likely, given the apparently smaller values of J_2 and J_3, that the cluster is not in the magnetic ground state at the measurement temperature of 1.9 K, so it not possible to assign a ground-state spin value for the cluster from this curve (Supporting Information, Figure 10S).

The magnetic susceptibility of **4** shows an increasing value on cooling, reaching 0.804 cm^3 mol^{-1} at 1.86 K (Figure 14). The inverse susceptibility plot shows non-linear behavior over the whole temperature range, so the Curie−Weiss fit

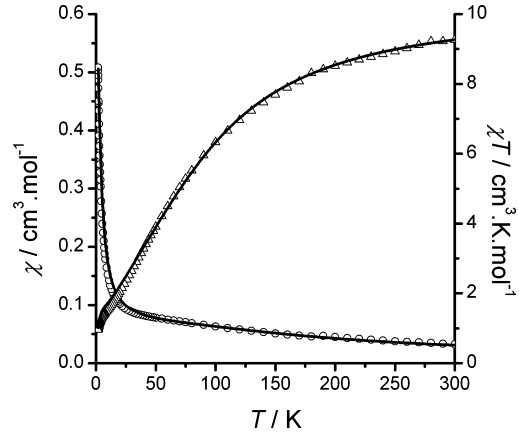

Figure 15. Plot of $\chi(T)$ (circles) for **5** with fit to the two-trimer model (red line) and $\chi T(T)$ (triangles) with fit (blue line) for $g = 1.99(1)$, $2J_1/k_B = +32.5(2)$ K, $2J_2/k_B = -16.8(1)$ K, and $2J_3/k_B = +0.4(1)$ K.

was not attempted. The $\chi T(T)$ plot (Figure 14) shows a decreasing product on cooling with a value at 300 K of 13.46 cm^3 K mol^{-1} which is close to the value expected for an uncoupled $Mn(II)_2Mn(III)_2$ system ($\chi T = 14.75$ for $g = 2.00$).

Compound **4** presents a better case for the use of the $J_2 = J_3$ model (Figure 13) as both clusters in the compound lack the additional carboxylate bridge through the d_{z^2} orbital of the Mn(III) atoms to the Mn(II) atoms. All superexchange pathways in **4** are through π-d interactions (Figure 12). The Mn(III)−Mn(III) distances are both 2.80(3) Å, which is longer than in **3** and accordingly, we see a weaker interaction as shown by the higher value of χT at 300 K.

The two clusters are crystallographically independent, yet also very similar in their Mn_4O_2 bond lengths and angles, so it is reasonable to apply the vector coupling model to this system if the clusters are to be taken as isolated systems. We are able to make a rough reproduction of the high temperature data using $g = 2.00$, $2J_1/k_B = -10$ K, and $2J_2/k_B = -5$ K, but it is likely that this is a significant oversimplification of the system as the bipyrimidine bridges will carry an interaction of the same order of magnitude as J_1 and J_2 and so will affect the data over the same temperature range as the intracluster couplings. The magnetization plot for **4** does not give any information regarding couplings as the measurement temperature of 1.9 K means that several states are likely to be significantly populated and the intercluster interactions through the chain will also affect this behavior strongly (Supporting Information, Figure 11S).

The magnetic susceptibility of **5** (Figure 15) increases with decreasing temperature from a value of 32.59×10^{-3} cm^3 mol^{-1} at 300 K to 508.1×10^{-3} cm^3 mol^{-1} at 1.86 K. The $\chi T(T)$ plot shows a decreasing value of χT on cooling with a value of 9.25 cm^3 K mol^{-1} at 300 K, which is somewhat lower than the spin-only value of 10.375 cm^3 K mol^{-1} for a non-interacting $Mn(II)Mn(III)_2$ species with $g = 2.00$. The inverse susceptibility curve shows non-linear behavior across the temperature range, so a Curie−Weiss fit was not attempted.

The high-temperature data (above 60 K) was modeled using a two-coupling system (Figure 16 and eq 6) which

gave $2J_1/k_B = +32.5(2)$ K, $2J_2/k_B = -16.8(1)$ K, and $g = 1.99(1)$.

$$H = -2J_1(S_A \cdot S_B) - 2J_2(S_A \cdot S_C + S_B \cdot S_C) \quad (6)$$

The coupling values derived from this fit indicate that the ground spin state of the individual clusters is $S = {}^3/_2$.

Despite the coupling between the trimers being a weak one through the hexamethylenetetramine, it causes the susceptibility below 50 K to differ from that of an isolated trimer. To model this behavior, we have made an approximation using two trimers coupled through Mn(III) (S_A and S_D) and Mn(II) (S_C and S_F) (Figure 16). Using the values of J_1 and J_2 obtained from the least-squares fitting of the isolated trimer model, we then used full-matrix diagonalization techniques to estimate the coupling between the trimers using the following Hamiltonian

$$H = -2J_1(S_A \cdot S_B + S_D \cdot S_E) - 2J_2(S_A \cdot S_C + S_B \cdot S_C + S_D \cdot S_F + S_E \cdot S_F) - 2J_3(S_C \cdot S_D + S_A \cdot S_F) \quad (7)$$

The best fit was obtained with $2J_3/k_B = +0.4(1)$ K.

Using the values obtained from the calculations, we can calculate a magnetization curve for this system (Supporting Information, Figure 12S). The calculation slightly overestimates the data, and the difference is higher than that expected from experimental error. A possible explanation is anisotropy around the Mn(III) atoms, which is usually to be expected, although it is likely that the model approximation causes this difference.

Experimental Section

Materials and Methods. All reactions were caried out under aerobic conditions using commercial grade solvents. $[Mn(O_2CCHMe_2)_2]$[8] was synthesized as described in reference 8. $[Mn(O_2CCMe_3)_2]$ was prepared as follows: $Mn(O_2CMe)_2 \cdot 4H_2O$ (2 g, 8.16 mmol) was heated in 10 mL of pivalic acid in an open system until the volume of the resulting solution was reduced by 40%. The solution was then allowed to cool to room temperature to afford a precipitate. The microcrystalline product was filtered off in several days, washed with hexane, and dried in air (Yield, 75%). Found C, 47.05; H, 7.29%. $Mn(O_2CCMe_3)_2 \cdot 4H_2O$ ($C_{10}H_{18}MnO_4$) requires C, 46.71; H, 7.06%. Organic ligands were purchased from commercial sources and used without further purification.

The infrared spectra were recorded on a Perkin-Elmer Spectrum One spectrometer using KBr pellets in the region 4000−400 cm^{-1}. Magnetic susceptibility measurements were made on a Quantum Designs MPMS SQUID-XL between 300−1.86 K in a field of 1000 G. Samples were prepared in gelatine capsules. Magnetization measurements were made at 1.9 K between 0−5 T. The susceptibility and magnetization data were corrected for diamagnetic contributions using Pascal's constants.[21]

X-ray Crystallography. Experimental data were collected on a Bruker APEX-2 diffractometer equipped with graphite-monochromatized Mo Kα radiation at 100 K for **1**, **2**, and **4** and at 150 K for **3** and **5**. Details of the crystal, data collection, and refinement parameters are in Table 7. After collection and integration the data were corrected for Lorentz and polarization effects and for absorption by semiempirical methods (SADABS).[22] The structures were solved by direct methods and refined by full-matrix least-squares on weighted F^2 values for all reflections using the SHELX suite of programs.[23] The non-hydrogen atoms were refined with anisotropic displacement parameters. In compound **2** solvate ethanol molecules are disordered over two positions with occupancies of 0.57/0.43. One of methyl groups (C11) of isobutyric acid in **4** was also disordered over two positions.

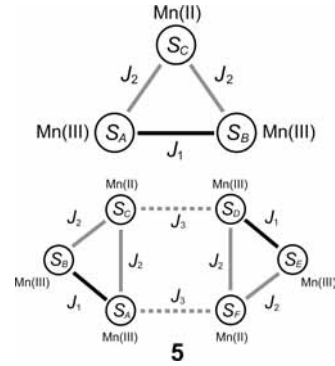

Figure 16. Schematic of the coupling system used for high-temperature fit (top) and to model all data (bottom) for **5**.

Synthesis of Complexes. $[Mn_3(O_2CCHMe_2)_6(dpa)_2] \cdot 2MeCN$ (1). To a solution of $Mn(O_2CCHMe_2)_2$ (0.11 g, 0.48 mmol) in 2.5 mL of EtOH was added a solution of 2,2′-dipyridylamine (0.08 g, 0.46 mmol) in 2.5 mL of MeCN. The resulting mixture was left undisturbed at room temperature. The yellow crystals of complex **1** suitable for X-ray analysis were separated by filtration, washed with MeCN, and dried in air (Yield, 0.11 g, 65%). Found C, 51.26; H, 6.03; N, 9.29%. Complex **1** ($C_{48}H_{66}Mn_3N_8O_{12}$) requires: C, 51.85; H, 5.98; N, 10.08%. IR (KBr, cm^{-1}): 3430br.m, 3324s, 3257sh, 3213s, 3149m, 3113m, 3044m, 2966vs, 2929sh, 2870sh, 1651sh, 1591sh, 1578vs, 1535sh, 1484vs, 1421vs, 1372s, 1284s, 1233m, 1158w, 1121w, 1093m, 1061w, 1006m, 926m, 852sh, 837m, 768s, 741sh, 640m, 556sh, 531m.

$([Mn_3(O_2CCHMe_2)_6(bpm)] \cdot 2EtOH)_n$ (2). To a solution of $Mn(O_2CCHMe_2)_2$ (0.046 g, 0.2 mmol) in 3 mL of EtOH was added a solution of 2,2′-bipyrimidine (0.016 g, 0.1 mmol) in 3 mL of CH_2Cl_2. The resulting mixture was left undisturbed at room temperature for several days. The yellow crystals of the title complex suitable for X-ray analysis were separated by filtration, washed with ether, and dried in air (Yield, 0.035 g, 56%). Found C, 45.93; H, 5.65; N, 5.48%. Complex **2** ($C_{36}H_{60}Mn_3N_4O_{14}$) requires C, 46.09; H, 6.45; N, 5.97%. IR (KBr, cm^{-1}): 3413br.m, 3083sh, 2970s, 2931sh, 2871sh, 1570vs, 1557sh, 1476s, 1423vs, 1384sh, 1374m, 1361sh, 1286m, 1218w, 1168w, 1147w, 1094m, 1018w, 926w, 840w, 783w, 762m, 736w, 689w, 664m, 553w, 533w.

$[Mn_4O_2(O_2CCMe_3)_6(bpy)_2]$ (3). To a solution of $Mn(O_2CCMe_3)_2$ (0.26 g, 1.01 mmol) in 5 mL of THF was added a solution of 2,2′-bipyridine (0.16 g, 1.02 mmol) in 5 mL of THF. The resulting mixture was left undisturbed at room temperature for 2 days. The brown crystals of the title complex suitable for X-ray analysis were separated by filtration, washed with THF, and dried in air (Yield, 0.19 g, 66%). Found C, 51.81; H, 6.09; N, 4.44%. Complex **3** ($C_{50}H_{70}Mn_4N_4O_{14}$) requires C, 51.3; H, 6.03; N, 4.79%. IR (KBr, cm^{-1}): 3437br.m, 2957m, 2926sh, 2870sh, 1591vs, 1551s, 1483s, 1444m, 1418s, 1371m, 1358sh, 1227m, 1016m, 792m, 765m, 740w, 656sh, 629m, 598sh.

$[Mn_4O_2(O_2CCHMe_2)_6(bpm)(EtOH)_4]_n$ (4). To a solution of $Mn(O_2CCHMe_2)_2$ (0.046 g, 0.2 mmol) in 2.5 mL of EtOH was added a solution of 2,2′-bipyrimidine (0.016 g, 0.1 mmol) in 2.5 mL of THF. The obtained solution was allowed to stand at room

(21) Kahn, O. *Molecular Magnetism*; Wiley VCH Publishers, Inc.: New York, 1993.

Table 7. Summary of Crystal, Data Collection, and Refinement Details

complex	$[Mn_3(O_2CCHMe_2)_6(dpa)_2]\cdot 2MeCN$ (**1**)	$([Mn_3(O_2CCHMe_2)_6(bpm)]\cdot 2EtOH)_n$ (**2**)	$[Mn_4O_2(O_2CCMe_3)_6(bpy)_2]$ (**3**)	$[Mn_4O_2(O_2CCHMe_2)_6(bpm)(EtOH)_4]_n$ (**4**)	$([Mn_3O(O_2CCHMe_2)_6(hmta)_2]\cdot EtOH)_n$ (**5**)
formula	$C_{48}H_{66}Mn_3N_8O_{12}$	$C_{36}H_{60}Mn_3N_4O_{14}$	$C_{100}H_{140}Mn_8N_8O_{28}$	$C_{60}H_{108}Mn_6N_6O_{27}$	$C_{38}H_{72}Mn_3N_8O_{14}$
molecular weight	1111.91	937.70	2341.72	1675.16	1029.86
T, K	100(2)	100(2)	150(2)	100(2)	150(2)
crystal system	orthorhombic	triclinic	monoclinic	triclinic	monoclinic
space group	*Pbca*	*P*$\bar{1}$	*C2/c*	*P*$\bar{1}$	*P*2(1)/*n*
a, Å	10.8949(5)	8.9434(4)	25.323(3)	12.0006(19)	14.9889(9)
b, Å	21.0389(10)	11.0838(5)	18.8482(18)	14.394(2)	20.6351(12)
c, Å	23.3902(11)	11.7545(6)	13.8931(14)	24.302(3)	15.7126(9)
α, deg	90	88.675(3)	90	105.381(11)	90
β, deg	90	72.588(3)	108.735(2)	95.296(11)	102.445(4)
γ, deg	90	84.840(3)	90	93.826(12)	90
V, Å^3	5361.4(4)	1107.28(9)	6279.7(11)	4011.9(11)	4745.7(5)
Z	4	1	2	2	4
ρ, mg m^{-3}	1.378	1.406	1.238	1.387	1.441
μ, mm^{-1}	0.761	0.907	0.843	0.991	0.856
crystal size, mm^3	0.50 × 0.17 × 0.06	0.37 × 0.24 × 0.07	0.40 × 0.32 × 0.14	0.40 × 0.20 × 0.04	0.22 × 0.15 × 0.08
theta range for data collection	1.74 to 25.00°	1.82 to 25.00°	1.37 to 25.00°	1.49 to 25.00°	1.65 to 25.00°
Index ranges	$-12 \le h \le 12$, $-25 \le k \le 25$, $-27 \le l \le 27$	$-10 \le h \le 10$, $-13 \le k \le 13$, $-13 \le l \le 13$	$-30 \le h \le 30$, $-22 \le k \le 22$, $-16 \le l \le 16$	$-14 \le h \le 14$, $-17 \le k \le 17$, $-28 \le l \le 28$	$-17 \le h \le 17$, $-23 \le k \le 22$, $-18 \le l \le 18$
reflections collected	85281	16364	22381	53130	46641
independent reflections	4715 [R(int) = 0.0906]	3870 [R(int) = 0.0334]	5538 [R(int) = 0.0613]	14109 [R(int) = 0.1781]	8096 [R(int) = 0.1080]
completeness to theta	100.0%	99.4%	100.0	99.9%	96.8%
data/restraints/parameters	4715/0/329	3870/7/276	5538/0/325	14109/1/921	8096/0/581
goodness-of-fit on F^2	1.041	1.022	1.053	0.979	1.005
final R_1, wR_2	0.0388, 0.0760	0.0414, 0.1118	0.0455, 0.1126	0.0695, 0.1219	0.0493, 0.0968
R indices (all data)	0.0563, 0.0828	0.0488, 0.1179	0.0655, 0.1244	0.2046, 0.1721	0.0997, 0.1181
largest diff. peak and hole, e Å^3	0.357 and −0.425	1.383 and −0.550	1.469 and −0.359	0.763 and −0.645	0.499 and −0.435

temperature for 2 weeks. The black crystals suitable for X-ray analysis were separated by filtration, washed with EtOH, and dried in air (Yield, 0.038 g, 68%). Found C, 42.81; H, 5.93; N, 4.77%. Complex **4** ($C_{40}H_{72}Mn_4N_4O_{18}$) requires C, 43.02; H, 6.50; N, 5.02%. IR (KBr, cm^{-1}): 3435br.m, 2969m, 2930sh, 2874sh, 1635sh, 1617sh, 1588sh, 1570vs, 1473m, 1421s, 1384m, 1286m, 1166m, 1096m, 1042w, 1017sh, 763w, 689sh, 656sh, 626m, 562sh, 508sh.

$([Mn_3O(O_2CCHMe_2)_6(hmta)_2]\cdot EtOH)_n$ (5). To a hot solution of $Mn(O_2CCHMe_2)_2$ (0.23 g, 1.00 mmol) in 10 mL of THF was added a hot solution of hexamethylenetetramine (0.28 g, 2.00 mmol) in 10 mL of EtOH. The obtained solution was allowed to cool to room temperature and left for some days. The black crystals suitable for X-ray analysis were separated by filtration, washed with EtOH and dried in air (Yield, 0.08 g, 22%). Found C, 44.35; H, 7.18; N, 10.52%. Complex **5** ($C_{38}H_{72}Mn_3N_8O_{14}$) requires C, 44.32; H, 7.05, N, 10.88%. IR (KBr, cm^{-1}): 3431br,m, 2967m, 2931sh, 2874sh, 1615vs, 1470s, 1416vs, 1368s, 1300m, 1283m, 1251s, 1231s, 1169m, 1093m, 1055m, 1025s, 996s, 925m, 900w, 840m, 798m, 764s, 712s, 680s, 661s, 555m.

Conclusions

Polypyridyl linkers such as bipyrimidine or hexamethylentetramine ligands have been used to bind the manganese clusters of different nuclearities into 1D coordination polymers. The prepared coordination polymers **2**, **4**, and **5**, as well as their precursor tri- and tetranuclear clusters **1** and **3**, have been structurally characterized. We find that using a combination of vector coupling and full-matrix diagonalization techniques enables us to make good estimates of the intercluster coupling in **2** and **5**, for which no model was previously reported. In addition to the preliminary magnetic investigation of the polymorphs of **3**, we will attempt the separation of the polymorphs to provide the susceptibility of each polymorph and also to provide a higher-quality structure for **3a** in a further publication.

Acknowledgment. This work was supported by the Swiss National Science Foundation (SCOPES 7MDPJ065712.01/1 and IB7320-110976/1).

Supporting Information Available: X-ray crystallographic data in CIF format for complexes $[Mn_3(O_2CCHMe_2)_6(dpa)_2]\cdot 2MeCN$ (**1**), $([Mn_3(O_2CCHMe_2)_6(bpm)]\cdot 2EtOH)_n$ (**2**), $[Mn_4O_2(O_2CCMe_3)_6(bpy)_2]$ (**3**), $[Mn_4O_2(O_2CCHMe_2)_6(bpm)(EtOH)_4]_n$ (**4**) and $([Mn_3O(O_2CCHMe_2)_6(hmta)_2]\cdot EtOH)_n$ (**5**), packing diagram for **1** (Figure 1S), **2** (Figure 2S), **3** (Figure 4S), **4** (Figure 6S), **5** (Figure 7S), a view of solvate molecules above and below the plane of bpm in **2** (Figure 3S), hydrogen bonding interactions in **4** (Table 2S), the asymmetric unit in **4** with a numbering scheme (Figure 5S), magnetization plots for **1**, **2**, **3**, **4**, and **5** (Figures 8S, 9S, 10S, 11S, and 12S, respectively), bond valence sum (BVS) calculations (Table 1S). This material is available free of charge via the Internet at http://pubs.acs.org. Crystallographic data have been deposited with Cambridge Crystallographic Data Centre under nos. CCDC 692808−692812 for compounds **1**−**5**. Copies of this information may be obtained from the Director, CCDC, 12 Union Road, Cambridge, CB2 1EZ, U.K. (fax: +44−1233−336033; e-mail: deposit@ccdc.cam.ac.uk or http://www.ccdc.cam.ac.uk).

IC8014145

(22) Sheldrick, G. M. *SADABS*, version 2.10; University of Göttingen: Göttingen, Germany, 2003.
(23) Sheldrick, G. M. *SHELXS-97 and SHELXL-97*; University of Göttingen: Göttingen, Germany, 2003.